Analysis of Noise Removal Techniques on Retinal Optical Coherence Tomography Images

T.M.Sheeba[1]
Research Scholar
Department of Computer Applications
College of Science and Humanities
SRM Institute of Science and Technology, Kattankulathur,
Chennai, India

Dr. S. Albert Antony Raj[2]
Associate Professor and Head
Department of Computer Applications
College of Science and Humanities
SRM Institute of Science and Technology, Kattankulathur,
Chennai, India

***Abstract*—In the biomedical field, automatic disease detection by image processing has become the norm in the current days. For early illness detection, ophthalmologists have explored a variety of invasive and noninvasive procedures. Optical Coherence Tomography (OCT) is a noninvasive imaging technique for obtaining high resolution tomographic images of biological systems. The image quality is degraded by noise, which degrades the performance of noisy image processing algorithms. The OCT images captured with speckle noise and prior to further processing, it is critical to use an effective approach for denoising the image. In this paper, we used Median filter, Average filter or Mean filter, Wiener filter, Gaussian filter and Bilateral filter on OCT images in this paper, and discussed the advantages and drawbacks of each approach. The effectiveness of these filters are compared using the Peak Signal to Noise Ratio (PSNR), Mean Square Error (MSE) and Contrast to Noise Ratio (CNR).**

***Keywords*—Average or Mean filter; Bilateral filter; denoising image; Gaussian Filter; Median filter; optical coherence tomography; Wiener filter**

I. INTRODUCTION

Many practitioners have recently embraced Optical Coherence Tomography (OCT) as a means of gathering data from the human eye in order to diagnose problems. In today's world, OCT is a well-known imaging technology that is used to monitor retinal illnesses in the medical industry. Although, during the data acquisition phase of OCT, a grainy prototype known as speckle noise is always present. The attendance of speckle noise in OCT images limits image processing, making patient diagnosis harder for a practitioner. Due to the attendance of speckle noise in OCT images, blood vessels and layer bounds appear to be disconnected. The working approach to obtain OCT images is nearly identical to that for collecting ultrasound images, with the exception of the medium utilised to obtain it. Fig. 1 shows the OCT images of human eye. In the OCT image acquisition technique, light beams are employed as an alternative of the sound beams used in ultrasound imaging [1]. OCT imaging has been shown to play a key responsibility in the diagnosis of disorders associated to the retina and glaucoma in the medical realm [2-4]. OCT is one of the greatest techniques in the medical sector for finding the inside structure of the retina and high- intention images of the retina [5-8]. It has been discovered via the observations of several specialists that retinal layer width improves experimental results in the field of optometrist. In the case of glaucoma development and macular degeneration, retinal layer segmentation also improves clinical findings. The speckle noise in OCT images degrades picture quality and reduces the image's contrast to noise ratio. A despeckle method is necessary as a pretreatment step in the denoising operation of OCT images to defeat the effect of speckle noise and to maintain the excellent details of the OCT images. Preprocessing OCT images is therefore a crucial step in ophthalmology to improve clinical findings. The motivation of this research work is to choose the best denoising method to reduce speckle noise in the retinal OCT images without removing the details in the image. We analysed the Median Filter, Gaussian Filter, Bilateral Filter, Wiener Filter, and Average or Mean Filter denoising methods on OCT images and proved the Wiener filter is the best denoising method to reduce speckle noise in retinal OCT images.

There are six sections in this paper. Introduction given in Section I, the brief description about the different types of noise is given in Section II, Section III contains denoising methods such as the Median Filter, Gaussian Filter, Bilateral Filter, Wiener Filter, and Average or Mean Filter, the implementation is given in Section IV and Section V discusses the performance measuring methods such as PSNR, CNR, and MSE, as well as how these measurements are used to evaluate results. Section VI concludes with a conclusion.

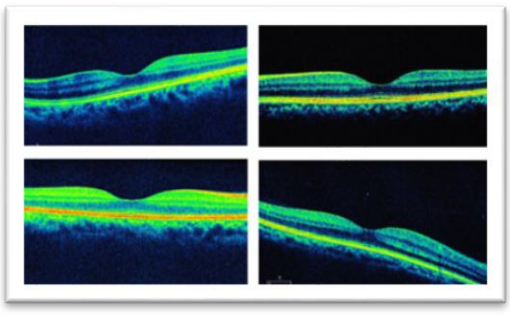

Fig. 1. OCT Images of Human Eye.

II. Literature Review

OCT is a technique that is frequently used to detect and track retinal conditions. However, despite technology advancements, speckle noise continues to significantly impair its scans. Speckle noise lowers the accuracy of measurements and the dependability of subsequent equipment. Mahnoosh Tajmirriahi et al. used a lightweight convolutional AE (Auto Encoders) used to simulate a recently developed state-of-the-art OCT picture denoising technique [9].

Xiaojun Yu et al. developed a two-step filtering method to reduce speckle noise, which consisting of Augmented Lagrange function minimization and Rayleigh alpha-trimmed filtering (AR) scheme. This mechanism examines the effects of speckle noise distributions on the OCT despeckling process [10].

Nahida Akter et al. proposed deep learning based method to remove noise from OCT images. The authors created and trained a U-Net model using OCT artifact-filled and artifact-free B-scans for investigation and shown that the U-Net performed better in terms of SSIM and PSNR values in removing the artefacts [11].

Bin Qiu et al. developed a deep network architecture. In the study, the authors used a most well-known frequently used modified DnCNN was used to denoise the OCT images [12].

Lirong Zeng et al. suggested progressive feature fusion attention dense network (PFFADN) for removing speckle noise from OCT images. In order to create a residual block, the authors sequentially connected the shallow and deep convolution feature maps that were retrieved from each dense block. This is done by arranging densely connected dense blocks in the deep convolution network [13].

Ling Chen et al., used the SC-based denoising database creation is the central component of the described approach, SC-DnCNN. Since FF-OCT images don't require registration before SC due to their unique image characteristics, they outperform point scanning OCT in terms of producing clear images. This method allows for the inclusion of both noisy and relatively clear images as training data, the embedding of a spatial adaptive mapping based on the compounding database, and the reduction of the effect of the speckle [14].

Yan Hu et al. provided an adaptive-SIN filtering technique to address the problem of minimising the noise in OCT images of various types. The suggested square-root transform converts the Poisson noise in the OCT pictures to the Gaussian noise in order to enable the best noise removal by the subsequent shearlet transform. The edge information in the photos as well as other image fine features may be preserved by the 3D shearlet transform [15].

III. Types of Noise

Unwanted information causes image quality to deteriorate. The type of noise there in the original image plays a crucial impact in the image noise removal procedure. Noise having a Gaussian, salt and pepper sharing corrupts typical images. Speckle noise, which is multiplicative in nature, is another example of a typical noise. The following sections detail the behaviour of each of these noises.

A. Gaussian Noise

Gaussian noise is geometric noise with a normal distribution probability density function, commonly known as Gaussian noise. That is, the noise's possible values are Gaussian-distributed. The noise with a Gaussian amplitude sharing is correctly defined as Gaussian noise [16].

B. Salt and Pepper Noise

Quick, unexpected perturbations in the image signal generate salt and pepper noise, which appears as at random dotted white or black pixels over the image. In salt and pepper noise, the black pixels appear in bright areas and brightly pixels appear in dark areas. Dead pixels, analogue to digital converter problems, and transmission bit mistakes can all contribute to this form of noise [16].

C. Speckle Noise

All fundamental aspects of logical imaging, particularly clinical ultra sound imaging, are affected by speckle noise. Sound processing of backscatter signals from several spread targets is the cause. Signals from basic scatters generate speckle noise. Speckle noise is referred to as texture in pharmaceutical literature, and it may include diagnostic information Smoothing the texture may be less desirable for visual interpretation. Physicians prefer the original noisy photos to the smoothed versions more willingly because the filter, even if it is more sophisticated, can eliminate some important image information. As a result, it's critical to create noise filters that maintain the traits that matter to doctors. To reduce speckle noise, several methods are utilised, each based on a distinct mathematical description of the phenomenon. For eliminate speckle noise in ultrasound pictures, we recommend hybrid filtering techniques [16].

IV. Filtering Techniques

A variety of filtering techniques are obtainable in the literature for the elimination of noise. Linear filtering techniques and non-linear filtering techniques are the two main categories. A linear-output filter's is the same as the input, whereas a non-linear-output filter's is different.

A. Mean Filter or Average Filter

The mean filter counts each pixel in a picture by replacing it with the mean or average value of its neighbours. So in the output image the pixel values that are out of character with their surroundings are deleted. It's built on a kernel, which, like other convolutions, represents the structure and width of the sampled neighbourhood when computing the mean. As shown in Fig. 2, a 3×3 kernel is commonly employed, but greater kernels, such as 5×5, may be utilised for more severe smoothing.

B. Median Filter

Median filtering is a nonlinear smoothing technique. Restore the value of each pixel with the median value of neighborhood element, which is better ordered for decreasing salt and pepper noise. That is, we choose a kernel and sort all elements in the neighbourhood by grey value, with the group's median acting as the output element for the neighbourhood centre. When an element in the proximity of other elements is

unusual, use the grey value of the elements in the field. That is the value that is halfway between the two extremes [17]. Take the field's element grey value when a element neighbourhood of element number is even. In the middle of two scales, it is the sort value. The median filter reduces noise while maintaining image edge clarity. When the window size is increased in median filtering, noise is successfully reduced [18].

$\frac{1}{9}$	$\frac{1}{9}$	$\frac{1}{9}$
$\frac{1}{9}$	$\frac{1}{9}$	$\frac{1}{9}$
$\frac{1}{9}$	$\frac{1}{9}$	$\frac{1}{9}$

Fig. 2. 3×3 Average Kernel Often used in Mean Filter.

C. Max and Min Filter

In max and min filter, it assigns a new value to each pixel in an image based on the greatest or smallest amount of value in the neighbourhood around that pixel. The filter's shape is represented by the neighbourhood. Contrast enhancement and normalization [19], texture description [20], edge detection [21-22], and thresholding [26] have all employed maximum and minimum filters. The filters are dilation and erosion counterparts with a grey value.

D. Gaussian Filter

Gaussian filters are thought to be the best time domain filters. It's a type of lowpass filter that isn't uniform. Such filters have a Gaussian impulse response, and Gaussian filters are those that have a Gaussian function. It has the shortest feasible grouping delay. The fundamental purpose of a Gaussian filter is to reduce distortion in lowest and highest signals [23]. A Gaussian obscure, also known as Gaussian smoothing is an after-effect of concealing a picture with a Gaussian capability in image processing. This Gaussian smoothing superintendent is usually a 2-D convolutional superintendent that is used to obfuscate images and remove subtle element and clamours. Gaussian filter is frequently more difficult with salt and pepper. When compared to other filters, one of the key disadvantages of the Gaussian filter is that it takes a long time. As a rule, Gaussian filters do not overshoot a stage work input while restricting the climb and fall times [24].

E. Bilateral Filter

The bilateral filter is defined as a loaded average of pixels, similar to the Gaussian convolution. The bilateral-filter, on the other hand, maintains edges by taking intensity variations into account. Bilateral filtering is based on the concept that two pixels are adjacent not only if they engage adjacent spatial regions, but also if their photometric ranges are comparable [25].

F. Wiener Filter

Inverse filtering, sometimes known as generalised inverse-filtering, is a technique for restoring deconvolution. Inverse-filtering or generalised inverse-filtering can be used to improve an image that is dim using a known lowpass filter. Conversely, inverse filtering is extremely intuitive to additive-noise. We can create a restoration method for each type of deterioration and then join them using the "one degradation at a time" technique. Inverse filtering and noise smoothing are most stable when Wiener filtering is used. It reduces additive noise while also inverting blurring. In terms of MSE, Wiener filtering is the best option. It minimizes the overall mean square error. A linear-estimation of the unique image is used in Wiener filtering. A probabilistic foundation underpins the procedure. The Wiener-filter in the Fourier-domain can be written as follows because of the orthogonal principle:

$$W(f_1, f_2) = \frac{H^*(f_1,f_2)S_{xx}(f_1,f_2)}{|h(f_1,f_2)|^2 S_{xx}(f_1,f_2)+S_{\eta\eta}(f_1,f_2)} \quad (1)$$

where S_{xx} $(f_1,f_2)+S_{\eta\eta}$ (f_1,f_2) are correspondingly value spectra of the initial image and the additive- noise, and $H(f_1,f_2)$ is the blurring- filter. As can be seen, the Wiener filter has two separate parts: a noise smoothing part and inverse-filtering part. It not only uses inverse filtering (highpass filtering) to deconvolve the data, but it also uses compression to reduce the noise (lowpass filtering).

V. Implementation

The implementation process of comparison is depicted in the block diagram, Fig. 3. On six separate OCT images of an eye, we employ five noise removal techniques: Mean or Average, Median, Bilateral, Gaussian, and Wiener filters, and the efficiency of each filter is evaluated using PSNR, CNR, and MSE values.

The filtering techniques are implemented using Python. The original images are converted into grayscale images and then the filtering techniques are applied on those grayscale images. The sample resultant filtered images are given in Fig. 4.

VI. Evaluation and Results

A. Mean-Squared-Error (MSE)

The MSE value is the Mean-squared-error between the enhanced image Y(I, j) and the actual image I(i, j), which for a high-quality image is negligible. The MSE of a given image of range M N is calculated as follows:

$$MSE = \frac{1}{MN}\sum_{i=0}^{M-1}\sum_{j=0}^{N-1}[I(i,j) - Y(i,j)]^2 \quad (2)$$

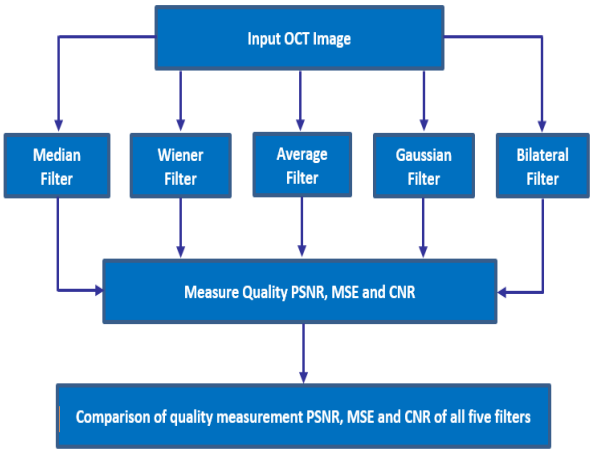

Fig. 3. Block Diagram of Implementation Process of Comparison.

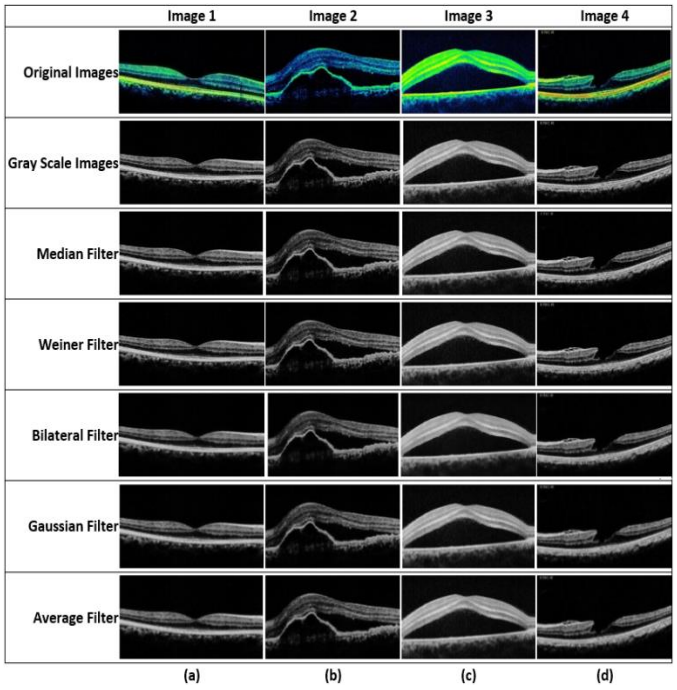

Fig. 4. Four Images are Passing through All Five Filtering Technique before and after, (a) OCT Image 1, (b) OCT Image 2, (c) OCT Image 3, (d) OCT Image 4.

It is determine by squaring the difference between the denoised (images after filtering) and noisy images and then taking the average of the difference [17]. Table I shows the MSE values of various filtered images. Fig. 5 shows the MSE graph after applying the median, wiener, bilateral, Gaussian, and average filters on all six images. Lower values of MSE specify improved image quality. When compared to the other four filters, Weiner has the lowest MSE value.

TABLE I. MSE VALUE OF FILTERED IMAGES

MSE Comparison						
Filters	**OCT Image 1**	**OCT Image 2**	**OCT Image 3**	**OCT Image 4**	**OCT Image 5**	**OCT Image 6**
Median	20.29753	21.86683	30.02484	20.54619	21.85792	27.43176
Weiner	**17.51171**	**19.10760**	**29.29777**	**17.57836**	**18.47427**	**26.82416**
Bilateral	26.06070	21.61373	39.38961	23.83720	19.67814	35.18031
Gaussian	27.99892	30.67310	45.20848	29.51530	29.22160	40.63345
Average	28.29255	31.12878	46.03533	29.96165	29.39583	41.33654

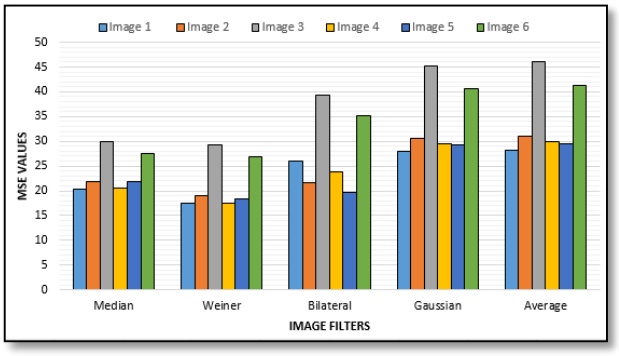

Fig. 5. Comparison of MSE Values of the Filtered Images.

B. Peak Signal-To-Noise Ratio (PSNR)

PSNR is defined as the relational of a signal's greatest value to the noise value that affects the signal's quality. PSNR is an image quality metric that provides a metric of noise that affects image quality. It determines the quantity of noise that has an impact on image quality. The image quality improves as the PSNR score rises. The PSNR value is calculated using the root-to- mean-square-error (RMSE), which is the square- root of the error between the input-image and the enhanced- image. For the largest possible pixel values, if RMSE will decrease, the PSNR will increase. As a result, greater PSNR values suggest better image improvement. PSNR has the advantage of being computationally and logically straightforward to optimise. One downside of root-mean-squared error is that it changes in lockstep with image intensity. PSNR's mathematical formulation is as follows:

$$PSNR = 10\log (S^2/MSE) \quad (3)$$

The greatest pixel value that can be assign in an image is S. For an 8-bit image, S=255. It can alternatively be defined as the ratio of greatest signal power to maximum noise power. This rate is expressed in decibels (dB). Table II shows the PSNR rate of all six images after going through various filters and Fig. 6 shows the comparison of PSNR values after applying the median, wiener, bilateral, Gaussian, and average filters on all six images. When compared to the other four filters, Weiner has the highest PSNR score.

TABLE II. PSNR VALUE OF FILTERED IMAGES

PSNR Comparison						
Filters	**OCT Image 1**	**OCT Image 2**	**OCT Image 3**	**OCT Image 4**	**OCT Image 5**	**OCT Image 6**
Median	35.0563 dB	34.7329 dB	33.3559 dB	35.0034 dB	34.7347 dB	33.7482 dB
Weiner	**35.6975 dB**	**35.3187 dB**	**33.3666 dB**	**35.6810 dB**	**35.4651 dB**	**33.8455 dB**
Bilateral	33.9709 dB	34.7835 dB	32.1769 dB	34.3582 dB	35.1909 dB	32.6678 dB
Gaussian	33.6593 dB	33.2632 dB	31.5786 dB	33.4303 dB	33.4737 dB	32.0419 dB
Average	33.6140 dB	33.1991 dB	31.4998 dB	33.3651 dB	33.4479 dB	31.9674 dB

C. Contrast to Noise Ratio (CNR)

CNR is a metric for determining the quality of an image. The measure SNR is a like to the CNR, with the exception that it subtracts a term before calculating the ratio [27]. When there is a considerable bias in an image, such as from haze [28], this is critical. The intensity is quite strong, as can be seen in the image to the right, even though the image's features are washed out by the haze. As a result, while this image has a higher SNR measure, it has a lower CNR measure. One method to define difference to noise rate is [29, 30]:

$$C = |S_A - S_B| / \sigma_o \quad (4)$$

S_A and S_B are signal strengths for signal produce structures A and B in the region of interest, while σ_o is the SD of the clean image noise. Table III shows the contrast to noise ratio of the six images after processing through various filters and Fig. 7 shows the CNR graph after applying the median, wiener, bilateral, Gaussian, and average filters on all six images. Lower values of CNR specify improved image quality. CNR value for Weiner is least as compare to other four filters.

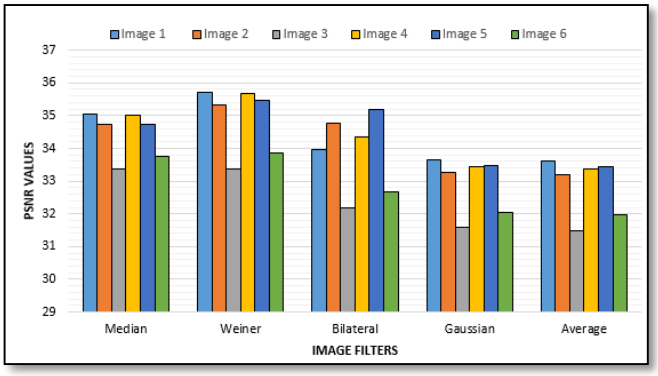

Fig. 6. Comparison of PSNR Values of the Filtered Images.

TABLE III. CNR VALUE OF FILTERED IMAGES

CNR Comparison						
Filters	**OCT Image 1**	**OCT Image 2**	**OCT Image 3**	**OCT Image 4**	**OCT Image 5**	**OCT Image 6**
Median	0.01458	0.02405	0.01017	0.01696	0.01680	0.01045
Weiner	**-0.00081**	**-0.00166**	**-0.00052**	**-0.00103**	**-0.00029**	**-0.00095**
Bilateral	0.01779	0.00892	0.00303	0.00484	0.00475	0.00244
Gaussian	0.00334	0.00436	0.00198	0.00359	0.00323	0.00217
Average	0.00345	0.00441	0.00203	0.00365	0.00332	0.00221

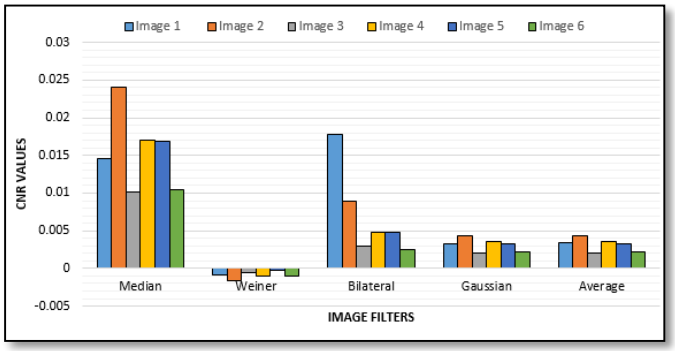

Fig. 7. Comparison of CNR Values of the Filtered Images.

VII. CONCLUSION

Due to the chaos in OCT images, ophthalmologists have difficulty in correctly detecting disease. It is also a barrier to the automatic segmentation of biomedical images for illness diagnosis. The Wiener filter functioned well on all six OCT images, according to the results in Section V. The Wiener filtering algorithm significantly decreases speckle noise, while also preserving retinal formation and reducing the stairway effect. Tables I, II, and III show that among the several despeckling filters evaluated here, the Wiener filtering algorithm is the most excellent way for reducing the produce of speckle noise while keeping the edges. Further, this work can be extended by analysing other denoising methods and quality matrices such as SSIM, SNR, ENL and MAE on retinal OCT images.

REFERENCES

[1] D. Huang, E. A. Swanson, C. P. Lin, J. S. Schuman, W. G. Stinson, W. Chang "Optical Coherence Tomography," Science, vol. 254, pp. 1178-1181, 1991.

[2] M. R. Hee, C. A. Puliafito, C. Wong, J. S. Duker, E. Reichel, B. Rutledg "Quantitative assessment of macular edema with optical coherence tomography," Archives of ophthalmology, vol. 113, pp. 1019-1029, 1995.

[3] R. Koprowski and Z. Wróbel, "Image processing in optical coherence tomography using Matlab", Poland: Katowice, 2011.

[4] A. G. Podoleanu, "Optical Coherence Tomography" The British Journal of Radiology, vol. 78, pp. 976-988, 2005.

[5] W. Drexler, J.G. Fujimoto, "Optical Coherence Tomography", Springer, 2008.

[6] Y. Chen, L.N. Vuong, J. Liu, J. Ho, V.J. Srinivasan, I. Gorczynska, A.J. Witkin, J.S. Duker, J. Schuman, J.G. Fujimoto "Three-dimensional ultra high resolution optical coherence tomography imaging of age-related macular degeneration", Opt. Express 17, pp. 4046–4060, 2009.

[7] I. Krebs, S. Hagen, W. Brannath, P. Haas, I. Womastek, G. deSalvo, S. Ansari-Shahrezaei, S. Binder "Repeatability and reproducibility of retinal thickness measurements by optical coherence tomography in age-related macular degeneration", Ophthalmology, 117, 1577–1584, 2010.

[8] M. Anand and Dr. C. Jayakumari, "Study of retina image segmentation algorithms from optical coherence tomography(OCT) images", Jour of Adv Research in Dynamical & Control Systems, Vol. 9, No. 4, pp. 125-134, 2017.

[9] M. Tajmirriahi, R. Kafieh, Z. Amini and H. Rabbani, "A lightweight mimic convolutional auto-encoder for denoising retinal optical coherence tomography images", in IEEE Transactions on Instrumentation and Measurement, Vol. 70, pp. 1-8, 2021.

[10] X. Yu, C. Ge, Z. Fu, M. Z. Aziz and L. Liu, "A two-step filtering mechanism for speckle noise reduction in OCT images," 2021 IEEE 9th International Conference on Information, Communication and Networks (ICICN), pp. 501-505, 2021.

[11] N. Akter, S. Perry, J. Fletcher, M. Simunovic and M. Roy, "Automated Artifacts and Noise Removal from Optical Coherence Tomography Images Using Deep Learning Technique," 2020 IEEE Symposium Series on Computational Intelligence (SSCI), pp. 2536-2542, 2020.

[12] Bin Qiu, Zhiyu Huang, Xi Liu, Xiangxi Meng, Yunfei You, Gangjun Liu, Kun Yang, Andreas Maier, Qiushi Ren and Yanye Lu, "Noise reduction in optical coherence tomography images using a deep neural network with perceptually-sensitive loss function", Biomedical Optics Express, Vol. 11, No. 2, pp. 817-830, 2020.

[13] L. Zeng, M. Huang, Y. Li, Q. Chen and H. -N. Dai, "Progressive Feature Fusion Attention Dense Network for Speckle Noise Removal in OCT Images," in IEEE/ACM Transactions on Computational Biology and Bioinformatics, 2022.

[14] I. -L. Chen, T. -S. Ho and C. -W. Lu, "Full Field Optical Coherence Tomography Image Denoising Using Deep Learning with Spatial Compounding," 2020 IEEE 17th International Symposium on Biomedical Imaging (ISBI), pp. 1975-1978, 2020.

[15] Yan Hu, Jianfeng Ren, Jianlong Yang , Ruibing Bai & Jiang Liu, "Noise reduction by adaptive SIN fltering for retinal OCT images", Scientific Reports 11, 19498, 2021.

[16] Sheikh Tania and Raghad Rowaida, "A Comparative Study of Various Image Filtering Techniques for Removing Various Noisy Pixels in Aerial Image", International Journal of Signal Processing, Image Processing and Pattern Recognition Vol.9, No.3, pp.113-124, 2016.

[17] R. Ramani, "The Pre-Processing Techniques for Breast Cancer Detection in Mammography Images", I.J. Image, Graphics and Signal Processing, Vol. 5, pp. 47-54, 2013.

[18] Rakesh M.R1, Ajeya B2, Mohan A., "Hybrid Median Filter for Impulse Noise Removal of an Image in Image Restoration", Research in Science, Vol. 3, Issue 3, 2014.

[19] Dorst, L., "Quantitative Analysis of Interferograms Using Image Processing Techniques", ICO-13 Conf. Digest, Sapporo, Japan 1984, pp. 476-477.

[20] Werman, M. and S. Peleg, "Min-Max Filters in Texture Analysis", IEEE PAMI-7, pp. 730- 733, 1986.

[21] Lee, J.S.J., R.M. Haralick and L.G. Shapiro, "Morphologic Edge Detection", Proc. 8th ICPR, Paris 1986, pp. 369-373.

[22] Van Vliet, L.J., I.T. Young and A.L.D. Beckers, "A Nonlinear Laplace Operator as Edge Detector in Noisy Images", submitted to CVGIP, 1987.

[23] Nithya. K, Aruna. A, Anandakumar. H, Anuradha. B, "A Survey On Image Denoising Methodology On Mammogram Images", International Journal of Scientific & Technology Research, Vol. 3, Issue 11, pp. 92-93, 2014.

[24] Kshema, M. J. George and D. A. S. Dhas, "Preprocessing filters for mammogram images: A review," 2017 Conference on Emerging Devices and Smart Systems (ICEDSS), pp. 1-7, 2017.

[25] Sylvain Paris, Pierre Kornprobst , Jack Tumblin, Fredo Durand , "A Gentle Introduction to Bilateral Filtering and its Applications", ACM Digital Library, 2007.

[26] Bernsen, J., "Dynamic Thresholding of Grey-Level Images", Proc. 8th ICPR, Paris 1986, pp. 1251- 1255.

[27] Welvaert, Marijke; Rosseel, Yves; Yacoub, Essa. "On the Definition of Signal-To-Noise Ratio and Contrast-To-Noise Ratio for fMRI Data", PLOS ONE. 8 (11): e77089 Bibcode: 2013.

[28] Jiang, Hou; Lu, Ning; Yao, Ling, "A High-Fidelity Haze Removal Method Based on HOT for Visible Remote Sensing Images". Remote Sensing. 8 (10): 844, pp. 1-18, 2016.

[29] Desai, Nikunj, "Practical Evaluation of Image Quality in Computed Radiographic (CR) Imaging Systems", Proceedings of SPIE - The International Society for Optical Engineering, 7622, 2010.

[30] Timischl F. The contrast-to-noise ratio for image quality evaluation in scanning electron microscopy, Scanning. 37 (1): 54-62, 2015.